

# Incremental Labeling of Voronoi Vertices for Shape Reconstruction

J. Peethambaran<sup>†1,4</sup> and A. Parakkat<sup>1</sup> and A. Tagliasacchi<sup>2</sup> and R. Wang<sup>3</sup> and R. Muthuganapathy<sup>1</sup>

<sup>1</sup>Department of Engineering Design, Indian Institute of Technology, Madras, India

<sup>2</sup>Department of Computer Science, University of Victoria, Canada

<sup>3</sup>Schulich School of Engineering, University of Calgary, Canada

<sup>4</sup>Department of Mathematics and Computing Science, Saint Mary's University, Canada

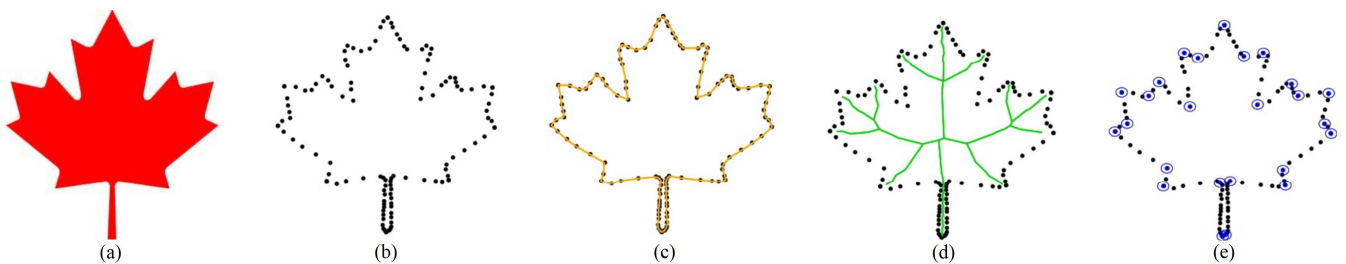


**Figure 1:** Shape representations generated by the proposed framework from non-uniform samples of Maple leaf boundary. (a) Representative image, (b) Point set (113 points), (c) Reconstructed Curve, (d) Medial axis (Interior) and (e) Dominant points (DP) shown in blue circles.

## Abstract

We present an incremental Voronoi vertex labeling algorithm for approximating contours, medial axes and dominant points (high curvature points) from two dimensional point sets. Though there exist many number of algorithms for reconstructing curves, medial axes or dominant points, a unified framework capable of approximating all the three in one place from points is missing in the literature. Our algorithm estimates the normals at each sample point through poles (farthest Voronoi vertices of a sample point) and use the estimated normals and the corresponding tangents to determine the spatial locations (inner or outer) of the Voronoi vertices with respect to the original curve. The vertex classification helps to construct a piece-wise linear approximation to the object boundary. We provide a theoretical analysis of the algorithm for points non-uniformly ( $\epsilon$ -sampling) sampled from simple, closed, concave and smooth curves. The proposed framework has been thoroughly evaluated for its usefulness using various test data. Results indicate that, even sparsely and non-uniformly sampled curves with outliers or collection of curves are faithfully reconstructed by the proposed algorithm.

## CCS Concepts

•Computing methodologies → Computer graphics; Shape analysis; •Theory of computation → Computational geometry;

## 1. Introduction

Recovering shape representations of an object from its boundary samples is a fundamental yet challenging problem in a number of fields such as computer graphics, computer vision, computational geometry, photogrammetry and reverse engineering [Lee00, Wan14, MBS16]. A handful of representations such as contours and skeletons, derived from the point set, provide valuable insights into the geometry of the corresponding object. These representative

geometric structures play a significant role in shape analysis, especially by boosting the computational performance and reducing the storage requirements. In this work, we develop a multi-purpose Voronoi based framework for extracting curves, medial axes and dominant points from non-uniform and possibly sparse data, sampled from the boundaries of geometric objects. Figure 1 showcases various shape representations extracted by the proposed framework from the points sampled along the contour of a maple leaf. Our shape representations range from highly detailed polygonal curves (Figure 1(c)) that span the input points to dominant points driven, coarse polygonal approximations (Figure 1(e)) that achieve high-

<sup>†</sup> jjjnair2000@gmail.com

level of data compression. Further, it also approximates medial axes (Figure 1(d)) of the object from its input samples.

Any simple closed curve divides the plane into a bounded and unbounded region. Voronoi vertices in the unbounded region can be labelled as *outer* while Voronoi vertices in the bounded region can be labelled *inner*. The labeling can give reasonable cues about various geometric structures representing the original curve. For instance, a Voronoi edge connecting *inner* and *outer* intersects the original curve. Consequently, its dual Delaunay edge can be used as a linear approximation to the corresponding curve portion. Similarly, all the Voronoi vertices lying in the bounded region approximate the interior medial axis, which can be captured via the corresponding dual Delaunay edges. While these observations are pretty standard in curve reconstruction domain and there have been many attempts to exploit these ideas in curve reconstruction, e.g. power crust [ACK01], a unified framework that handles curves, medial axes and high curvature points (referred to as dominant points) is surprisingly missing in the literature.

We introduce a simple incremental Voronoi vertex labeling algorithm to extract these shape representations from points sampled from simple closed curves. Our algorithm heuristically computes the poles at each input sample, where the poles estimates the normals at samples [DW01]. Then, it uses these estimated normals and tangents at sample points along with the Voronoi branching pattern for the vertex classification and subsequently construct a piece-wise linear approximation to the boundary and the interior medial axis of the original curve. Extreme curvature portions induce specific labeling patterns of the voronoi diagram and these labeling patterns are utilized to identify dominant points on the input curve. A theoretical evaluation of the incremental labeling algorithm for smooth curves is provided under  $\epsilon$ -sampling model [ABE98] and we demonstrate the practical potentials of the algorithm via several experiments and comparison with the state-of-the-arts.

## 2. Related Work

In this section, we briefly review the existing literature on curve reconstruction, medial axis extraction and dominant point identification in two-dimensions.

### 2.1. Curve Reconstruction

Over the past few decades, a number of approaches have been proposed for curve reconstruction. Curve reconstruction deals with the task of constructing a polygonal chain faithful to the original curve from its sample data. Most often, input data, acquired through sensors or extracted from images, consists of noise or outliers. These defect-laden data often pose a great challenge to the curve reconstruction problem. A few methods [Lee00, Wan14, CFG\*05, dGCSAD11] can deal with the reconstruction of curves from noisy input data. However, most of the Delaunay/Voronoi based reconstruction techniques interpolate the input data and consequently are less tolerant to noise.

Curve reconstruction from an arbitrary data, insufficiently sampled from an unknown original curve, is highly infeasible [ABE98]. A few conditions on the sampling are needed to guarantee a faithful reconstruction of the original curve. Under uniform sampling,

where the adjacent points are sampled at a distance less than a threshold value, many algorithms such as  $\alpha$ -shape [EKS83] and  $r$ -regular shapes [Att98] are known to work with reasonable accuracy. However, uniform sampling condition leads to dense sampling all over the curve, including the areas where a sparse sampling would be sufficient.

To capture the local level of details at each point sampled on a smooth curve, highly detailed portions of the curve demand a dense sampling whereas the portions that encapsulate less details, can be less densely sampled. Based on this observation, Amenta, Bern and Eppstein [ABE98] introduced a non-uniform sampling model called  $\epsilon$ -sampling (Definition 4), where the sampling density varies with the *local feature size* on the curve. Using the idea of  $\epsilon$ -sampling, they proposed *crust* algorithm which guarantees to construct a piece-wise linear approximation to a smooth curve, for certain  $\epsilon < 0.252$ . Subsequently, a few variants of *crust* such as nearest neighbor *crust* [DK99] and a locally defined *crust* [Gol99] were proposed. It is remarkable that nearest neighbor *crust* algorithm, though very simple in conception, improved the value of  $\epsilon$  to 0.333 from 0.252. Later, conservative *crust* [DMR00], that reconstructs a collection of open and closed smooth curves was described. Compared to the previous *crust* algorithms, conservative *crust* showed better resistance towards noise and outliers at the expense of a parameter tuning.

*Crust* and its variants fail in theory as well as in practice, for curves with sharp corners [DW02]. Using a different sampling condition for corner areas, Giesen [Gie99] showed that the traveling salesman tour of a point set densely sampled from a single closed curve  $\Sigma$  (possibly with corners), represents the correct reconstruction of  $\Sigma$ . In his work, the tangents (left and right) at any point on the curve must make a non-zero angle for a guaranteed reconstruction. By formulating traveling salesman problem in terms of a linear program and applying the ellipsoid method, Althaus and Mehlhorn [AM01] showed that the traveling salesman tour can be found in polynomial time for curve reconstruction. Dey and Wenger [DW01] described a heuristic called *gathan* that handles corners and endpoints and subsequently, in [DW02], they extended 'gathan' to reconstruct a collection of piece-wise smooth closed curves with provable guarantee. Funke and Ramos [FR01] introduced the concept of angular sampling where the angle determined by any edge  $(p_1, p_2)$  in the correct reconstruction and any other sample point  $p_3$  is upper bounded by a constant,  $\theta_{angle}$ . Under this sampling, they proposed an algorithm based on empty  $\beta$ -balls to handle a collection of curves with corners and end points.

Despite two decades of research, curve reconstruction is still an active problem among the computational geometry and computer graphics research communities. Recent research trends targets aspects such as improved sampling conditions [OMW16], reconstructing from fewer number of samples and curves with sharp corners [OM13], reconstruction from unstructured and noisy point cloud [OW18], unified frameworks for curve and shape reconstruction [MPM15], and applications of curve reconstruction to hand drawn sketches [PM16]. The proposed algorithm is a modified extension of the water flow based labeling algorithm proposed in [PPM15]. Compared to [PPM15], we have described the labeling framework in a formal setting with an additional technique for

dominant point detection and the algorithm has been validated using extensive experiments.

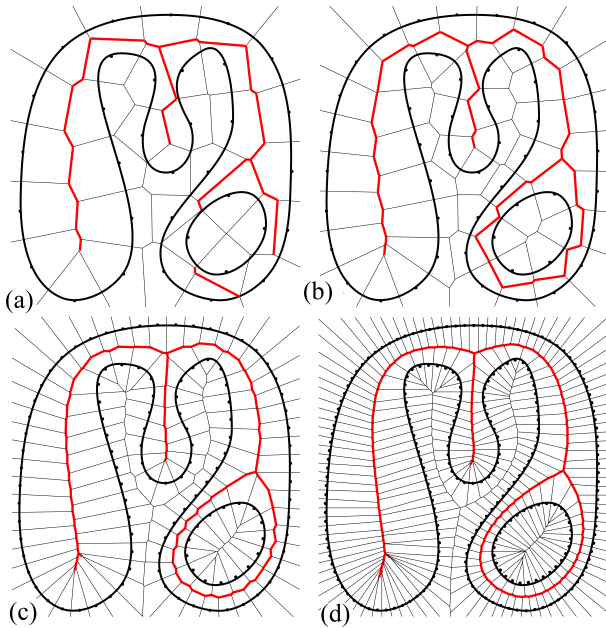


**Figure 2:** Relation between medial axis and Voronoi diagram. As the sampling rate increases, the Voronoi vertices converge to the medial axis. [Image courtesy: [TDS\* 16]]

### 2.2. Medial Axis Approximation

The *medial axis* of a curve  $C$  is defined as closure of the set of points in the plane which have two or more closest points in  $C$  [ABE98]. It is a powerful shape descriptor, widely used in shape analysis and feature extraction [FEC02]. Approximating the medial axis from the Voronoi diagram of points sampled along the boundary of objects has been addressed in [Gol99, FEC02, BA92, Bra94, GMP07a, ACK01, AK01, AM97]. Brandt and Algazi [BA92, Bra94] showed the relationship between the medial axis of a continuous regular shape and the Voronoi diagram of the points sampled along the border of the shape. Later, Fabbri et al. [FEC02] proved that all Voronoi vertices are also medial axis points (refer to Figure 2). More recent techniques generate the medial axis by minimizing the quadric error [LWS\* 15] or one-sided Hausdorff distance [ZSC\* 14] between the input shapes and the medial spheres. The research on medial axis computation from defect laden point clouds is still active, e.g. [ZC18] proposed an algorithm to construct compact medial axis from noisy and or occluded point clouds via approximating the signed distance function by a sparse optimization technique. A recent survey on medial skeletons providing formal definitions, a taxonomy of 3D skeletons and 3D shape skeletonization can be found in [TDS\* 16]. In our method, the set of *inner* Voronoi vertices obtained as a result of Voronoi vertex labeling approximates the interior medial axis of  $C$  (as shown in Figure 1(d)). We observe that our medial axis approximation is related to the union of inner

Voronoi balls centered at Voronoi vertices. Hence the theory developed in [GMP07a] is equally applicable to the proposed medial axis extraction.

### 2.3. Dominant Point Detection

In [Att54], Attneave observes that “the information on a curve is concentrated at points where the curve changes direction most rapidly”. This seminal observation led to many other subsequent approaches for finding the curvature extrema on the boundary of a planar object, see Figure 1(e). These extrema, commonly known as *dominant points (DP)*, can suitably describe the curve for both visual perception and recognition [Wu02].

Research on dominant points primarily focused on highly compressed linear polygons (obtained through DPs) that best approximate the input shape. In general, polygonal approximation techniques based on dominant points fall in one of the three categories: sequential approaches, split-and-merge approaches and heuristic approaches [Mas08]. Sequential approaches employ ideas such as longest possible line segments with minimum possible errors [RR93], region of support of each point [TC89, MS03] or min-max technique [KD82]. Split-and-merge approaches mainly differ in the manner that the curve has been split and this splitting procedure range from boundary segmentation [Ram72] through cornerity index [GDN04] to slope difference [HAA94]. Heuristic approaches for polygonal approximations mainly use either dynamic programming [Dun86, Sat92] or genetic algorithms [HS99, PNK98, YIN99]. Existing methods, mostly proposed in pattern recognition domain, target at polygonal approximation of digital curves. Conversely, we adopt a computational geometry approach to extract high curvature points from non-uniform boundary samples of known/unknown geometric objects.

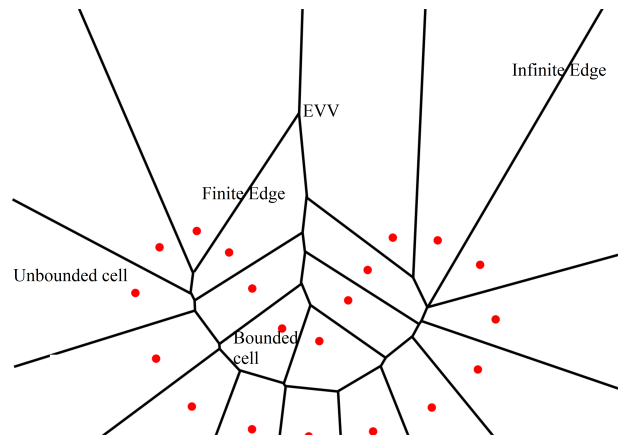


**Figure 3:** Voronoi diagram of a set of curve samples

### 3. Algorithm

We begin by defining the fundamental geometric structure, i.e., the Voronoi diagram, upon which the entire algorithm is designed, and introduce a few terminology relevant for discussing the incremental labeling algorithm.

### 3.1. Definitions and Notations

Let  $\mathcal{C}$  be a smooth, simple and closed curve (1-manifold) embedded in  $\mathbb{R}^2$ . Let  $P$  be a set of  $n$  points sampled from  $\mathcal{C}$  and  $\text{Conv}(P)$  denotes the convex hull of  $S$ . Further,  $d(p, q) = \|p - q\|$ , denotes the Euclidean distance between two points  $p, q \in P$ .

**DEFINITION 1** Voronoi cell ( $V_p$ ) [O'R98]:

A Voronoi cell of  $p \in P$  is the set of all points in the plane that are closer (or at least equidistant) to  $p$  than any other point in  $P$ :

$$V_p = \{x \in \mathbb{R}^2 \mid d(p, x) \leq d(q, x), \text{ where } p \neq q, \forall q \in P\}$$

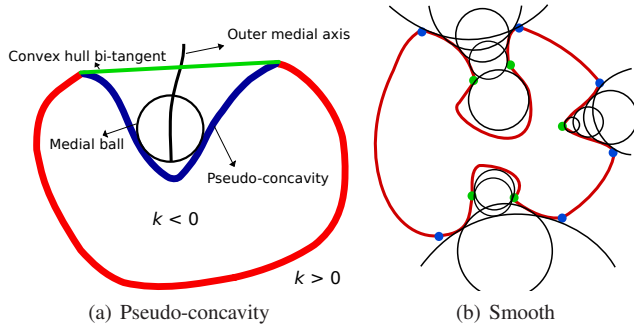


**Figure 4:** Illustration of pseudo-concavity and bi-tangent neighborhood portions of a simple closed curve in 2D. In Figure 4(b), pseudo-concave portions between blue and green points represent the bi-tangent neighborhood convergent (BNC) portions.

**Voronoi diagram (VD)** of  $P$ , denoted by  $\text{Vor}(P)$  is the subdivision of the plane into Voronoi cells with one cell  $V_p$  for each point  $p \in P$ . The locus of points on the plane that are equidistant from exactly two points,  $p$  and  $q$  is called a *Voronoi bisector* and a point that is equidistant to three or more points in  $P$  is called a *Voronoi vertex*. A simply connected subset of Voronoi bisectors is called a *Voronoi edge*. The VD consists of bounded and unbounded voronoi cells. A cell  $V_p$  is unbounded if the sample  $p$  lies on the convex hull of  $P$ . Unbounded Voronoi cells induce what is called as infinite edges, whose one vertex lies at infinity. All Voronoi vertices except the vertex at infinity are *finite*. We use the term *Extreme Voronoi Vertex (EVV)* to refer to the finite Voronoi vertex of an infinite Voronoi edge (refer to Figure 3). Observation 1 states a property of EVV which is exploited in the proposed incremental labeling.

**OBSERVATION 1** An extreme Voronoi vertex of a Voronoi diagram always belongs to two unbounded and one bounded voronoi cells

**DEFINITION 2** Delaunay triangulation ( $\text{Del}(P)$ ) [O'R98]:

The straight line dual graph of  $\text{Vor}(P)$  results in a planar triangulation called as Delaunay triangulation of  $P$ ,  $\text{Del}(P)$ .

**Pseudo-concavity.** We assume that  $\mathcal{C}$  is positively oriented (counter clockwise) closed, smooth and simple curve in 2D (refer to Figure 4(a)). A *medial ball*  $B(c, r)$ , centered at  $c \in$  medial axis of  $\mathcal{C}$  with radius  $r$ , is a maximal ball whose interior contains no points of  $\mathcal{C}$  [ABE98]. Let  $E$  be the set of all open connected regions of  $\text{Conv}(\mathcal{C}) \setminus \mathcal{C}$ . Each region given by the closure  $\bar{E}$ , is defined as a *pseudo-concave region ( $\mathcal{PC}_R$ )* of  $\mathcal{C}$  (Figure 4(a)). The portion of  $\mathcal{C}$  in each  $\mathcal{PC}_R$  is called *pseudo-concavity*, denoted by  $\mathcal{PC}$ . The edges

of  $\text{Conv}(\mathcal{C})$  in each *pseudo-concave region* are called *convex hull bi-tangents ( $BT_{\text{cvx}}$ )*. Every pseudo-concavity is capped by exactly one convex hull bi-tangent.

The curve  $\mathcal{C}$  is closed and concave and therefore, consists of convex and concave portions. We consider two sets, a concave set  $\mathcal{C}_{\text{ccv}}$  consisting of all the pseudo concavities of  $\mathcal{C}$  and a pseudo-convex set  $\mathcal{C}_{\text{cvx}}$ , containing all the portions of  $\mathcal{C}$  except  $\mathcal{C}_{\text{ccv}}$ , i.e.  $\mathcal{C} \setminus \mathcal{C}_{\text{ccv}}$ . Note that the intersection of  $\mathcal{C}_{\text{cvx}}$  and  $\mathcal{C}_{\text{ccv}}$  consists of bi-tangent points belonging to  $\text{Conv}(\mathcal{C})$ .

**Bi-tangent Neighborhoods.** Based on the radii of medial balls [ABE98], we characterize a property of the curve portions of  $\mathcal{C}$ , lying in the vicinity of the bi-tangents. The medial balls of a pseudo-concavity,  $\mathcal{C}$  tend to increase or decrease as it traverses through the outer MA lying in  $\mathcal{C}_R$ . The region in  $\mathcal{PC}_R$ , where the medial ball monotonically increases or decreases is defined as a *rolling interval* of the medial ball.

**DEFINITION 3 Bi-tangent neighborhood convergence (BNC):**

Bi-tangent neighborhoods of a pseudo-concavity,  $\mathcal{C}$  is said to be convergent, if the radius of the medial ball decreases monotonically in the first rolling interval, as it rolls along the outer MA of  $\mathcal{C}$  from the convex hull bi-tangent end to its interior.

In the case of smooth, concave and closed curves, viewed from the convex hull bi-tangent end, one can observe that the curves leading to the interior of  $\mathcal{C}$  in the neighborhood of convex hull bi-tangent, appears to be always converging. Figure 4(b) shows an example of BNC concave curve with a few pseudo concavities, each having a rolling interval (the curve portions between the bi-tangent points (blue colored) and the red points) where the radii of its medial ball decreases as it rolls along the corresponding outer MA from the convex hull bi-tangent.

**Sampling Condition.** Most of the reconstruction algorithms impose certain criteria on the sampling in order to provide theoretical guarantees on the reconstruction. A widely used sampling criteria is  $\epsilon$ -sampling [ABE98], where the sample spacing along the curve is determined by the local feature size (lfs) of the input curve (lfs of samples in particular). *Local feature size* at a point  $p$  on  $\mathcal{C}$ ,  $LFS(p)$  is the distance from  $p$  to the closest point on the medial axis of  $\mathcal{C}$ . A formal definition of  $\epsilon$ -sampling follows:

**DEFINITION 4**  $\epsilon$ -sampling [ABE98]: For a constant  $\epsilon > 0$ ,  $\mathcal{C}$  is said to be  $\epsilon$ -sampled by a finite set of samples  $P$ , if  $\forall p \in \mathcal{C}, \exists s \in P$  such that  $\|p - s\| \leq \epsilon LFS(p)$ .

### 3.2. Incremental Labeling in Pseudo-concavities

In any closed curve, concave components pose great challenges for reconstruction. Hence, we explain the labeling procedure by taking a concave portion of a simple closed curve. Labeling for convex curves is rather simple and direct. All the voronoi vertices are initially labelled as *outer* (illustrated using the dark blue blue points in Figure 5(a)). Incremental labeling in a pseudo-concavity starts with a EVV. Under dense sampling, each pseudo-concavity has at least one EVV lying outside the  $\text{Conv}(P)$  as established in Lemma 3.1. An extreme Voronoi vertex (EVV) has exactly two unbounded Voronoi cells due to the infinite edge and one bounded Voronoi cell

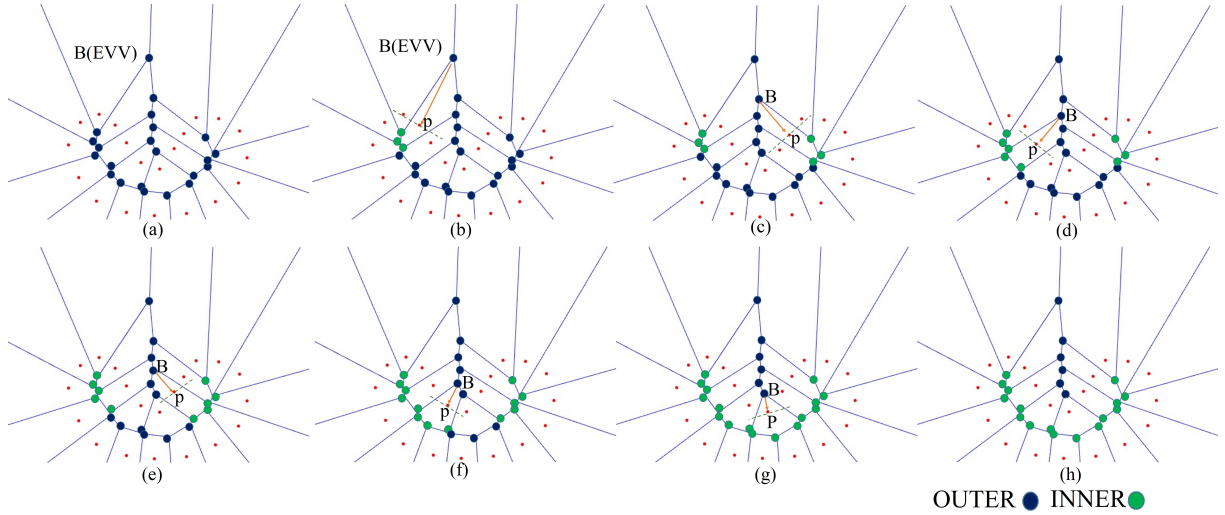


**Figure 5:** Illustration of incremental labeling in a concave portion of a closed planar curve. In the figure, red dots constitute the input points sampled from the curve, green and dark blue vertices respectively represent the inner and outer (w.r.t original curve) Voronoi vertices in the classification. Incremental labeling starts from a EVV and progresses towards the high curvature points in the concavity

adjacent to it (OBSERVATION 1). The EVV is paired with the sample of its adjacent bounded cell. Starting from the EVV the labeling process progresses to any unvisited *outer* Voronoi vertex adjacent to it. A few *outer* Voronoi vertices undergo label transitions from *outer* to *inner* during the incremental labeling process.

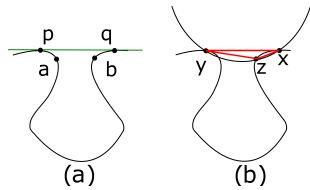


**Figure 6:** Illustration of Lemma 3.1.

**LEMMA 3.1**  $Vor(P)$ , where  $P$  is densely sampled ( $\epsilon$ -sample) from a smooth, closed, pseudo-concave and planar curve  $C$ , has at least one finite Voronoi vertex outside  $Conv(P)$

*Proof* Without loss of generality, we consider the bi-tangent neighborhood convergent portions (definition 3),  $\widehat{qb}$  and  $\widehat{ap}$  of a pseudo-concavity  $C$ , in the counter-clockwise direction of  $C$  (Figure 6 (a)). Let  $\widehat{xy}$  constitutes the convex hull edge capping  $C$  where  $x \in P$  and  $y \in P$  are either  $p$  and/or  $q$  or neighborhood points of  $p$  and/or  $q$  (refer to Figure 6 (b)). Let  $z \in P$  be the sample belonging to either  $\widehat{qb}$  or  $\widehat{ap}$  that is closest to either  $x$  or  $y$ . Under a dense sampling, an empty circle passing through  $x, y$  and  $z$  is always possible whose circum-center lies outside  $Conv(P)$  (shown in Figure 6 (b)) and hence the lemma.  $\square$

The condition that triggers the label transition of a Voronoi vertex is based on the normal estimation technique proposed in [AB98]. Amenta and Bern [AB98] observed that Voronoi cells of  $P$ , where  $P$  is  $\epsilon$ -sampled from a curve,  $C$ , tend to elongate in the

direction of the normal at each point. In [AB98], the authors define *poles*, which are two extreme Voronoi vertices of  $V_p$ , for each sample point  $p$ . In the case of curves, the reason for which the line passing through  $p$  and any of the two poles estimates the normal at  $p$  is explained in [DW01].

For a Voronoi cell  $V_p$  of a sample point, the outer Voronoi vertex where the labeling process starts, represents its source Voronoi vertex (SVV). Each sample  $p$  in  $P$  has its own Voronoi cell  $V_p$ , and hence one of the vertices of  $V_p$  subjected to the labeling procedure, is guaranteed to be the SVV of  $p$ .

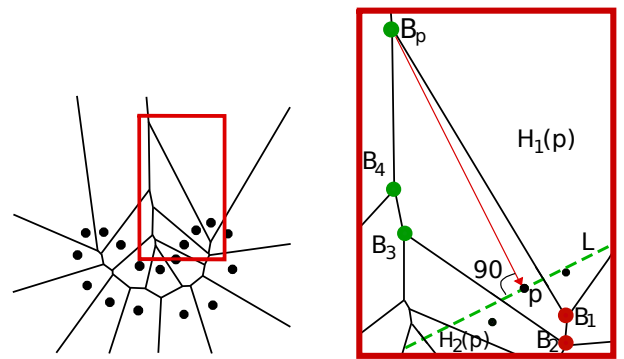


**Figure 7:** A bounded Voronoi cell with the normal (red line with arrow) and the tangent (green colored dashed line) of the sample, outer (green points), and inner (red points) Voronoi vertices.

Consider a bounded Voronoi cell  $V_p$  and its source Voronoi vertex (represented as  $B_p$ ) along with its owner point  $p$  as shown in Figure 7. The line  $L$ , orthogonal to  $\overrightarrow{B_p, p}$  divides the plane into two half planes designated as  $H_1(p)$  and  $H_2(p)$ . Using the vector,

$(B_p - p)$  and  $L$ , we present the state transition rule for a Voronoi vertex in our model in Definition 5.

**DEFINITION 5** Label transition rule:

Let  $B_i$  be an *outer* Voronoi vertex of a Voronoi cell  $V_p$  of a sample point  $p$  and  $B_p$  be the source Voronoi vertex of  $V_p$ ,  $B_i$  is labelled as *inner* if  $B_p$  and  $B_i$  lie on either side of  $L$

---

**Algorithm 1:** IncrementalLabel( $B$ )

---

**Input:** Branch Voronoi vertex,  $B$

- 1 Let  $p$  be the unpaired sample in the three Voronoi cells of  $B$ ;
- 2 Pair  $p$  with  $B$ ;
- 3 Apply state transition rule (Definition 5) to  $B$  in  $V_p$ ;
- 4 **if** there are no neighboring outer and unvisited vertices for  $B$   
    **then**
- 5 |   **return**;
- 6 **end**
- 7 **else if** there is one neighboring outer and unvisited vertex for  
     $B$  **then**
- 8 |   Let  $B_{new}$  be the outer neighboring vertex of  $B$ ;
- 9 |   IncrementalLabel( $B_{new}$ );
- 10 **end**
- 11 **else**
- 12 |   Let  $B_{new1}$  and  $B_{new2}$  be the outer neighboring vertices of  
     $B$ ;
- 13 |   IncrementalLabel( $B_{new1}$ );
- 14 |   IncrementalLabel( $B_{new2}$ );
- 15 **end**

---

Essentially, the source vertices estimates the poles of the samples as established in Lemma 3.2 and consequently, the vector,  $(B_p - p)$  and  $L$  approximates the normal and tangent at  $p$ , respectively. So, all the Voronoi vertices of  $V_p$  beyond  $p$  when viewed from  $B_p$  are labelled as *inner*. The justification is that the Voronoi vertices lying beyond the estimated tangent  $L$  of  $p$  also lie inside the original curve and hence can be considered as *inner*. The labeling algorithm advances to any neighboring unvisited outer Voronoi vertices of  $B_p$  (Figures 5(c)-5(f)) and is repeated until there are no neighboring unvisited outer Voronoi vertices for the current  $B_p$  (refer to Figure 5(g)). The incremental labeling in pseudo-concavities is presented in Algorithm 1. While the first recursive call (Line 7 of Algorithm 1) helps to traverse a single Voronoi branching, the second recursive call (Lines 11 and 12 of Algorithm 1) helps to traverse the two new Voronoi branchings corresponding to two inner pseudo-concavities. All the Voronoi vertices are visited exactly once during the Incremental\_Label() on  $B_p$ .

**LEMMA 3.2** In  $Vor(P)$ , where  $P$  is  $\epsilon$ -sampled from a smooth, concave and closed planar curve  $\mathcal{C}$ , source Voronoi vertex ( $B_p$ ) of a sample point  $p$  represents one of the poles of  $p$

*Proof* Amenta et al. [AB98] has observed that the poles of the Voronoi diagram of a sampling of a smooth curve converge to the medial axis. Hence, under dense sampling (as  $\epsilon$  approaches to zero) the positive pole of each sample lies on the exterior medial axis. The incremental labeling procedure starts with the EVV of a pseudo-concavity and EVV approximates one of the points in the exterior medial axis. Hence, EVV represents the positive pole of the

sample from its bounded Voronoi cell. As the transition rule (Definition 5) restricts the labeling procedure to the pseudo-concave region, i.e. the labeling advances only along the Voronoi vertices from the exterior medial axis of the pseudo-concave region, all the source Voronoi vertices obtained through such a labeling represent the poles of samples along the pseudo-concave curve portion.  $\square$

---

**Algorithm 2:** ExtractShapes( $P$ )

---

**Input:** Point set  $P$   
**Output:**  $curve(P)$

- 1 Construct  $Vor(P)$  and its dual  $Del(P)$ ;
- 2 Label all the vertices of  $Vor(P)$  including the INFINITE vertex to outer;
- 3 Pair up the samples in unbounded Voronoi cells with INFINITE vertex;
- 4 Construct a heap priority queue, PQ containing EVVs lying outside the convex hull of  $P$ , sorted in the descending order of their circum radii of the dual Delaunay triangles;
- 5 **while** PQ not empty **do**
- 6 |    $B = \text{root}(PQ)$ , delete  $B$  from PQ;
- 7 |   Incremental\_Label( $B$ );
- 8 **end**
- 9 Extract the graph,  $curve(P) = \{e \mid \text{edge } e \in Del(P) \text{ and } Dual(e) \text{ has outer and inner vertices}\}$ ;
- 10 Extract the graph,  $MAT(P) = \{e \mid \text{edge } e \in Vor(P) \text{ and } e \text{ has either two inner or outer vertices}\}$ ;
- 11 **return**  $curve(P)$ ;

---

We would like to point out that a similar labelling approach has been adopted in [GMP07b], to compute the medial axis (MA) of the union of inner Voronoi balls. However, the method proposed in [GMP07b] depends on a locally defined crust [Gol99], for the classification of Voronoi vertices. As opposed to this, the Voronoi vertex labelling in our approach is based on an incremental approach and hence in addition to the MA approximation, our method is also capable of reconstructing the boundary of the input sample.

### 3.3. Curve and Medial Axes Extraction

We assume that no four points are co-circular and hence each finite Voronoi vertex has a degree of 3. A pseudo code for curve reconstruction is provided in Algorithm 2. It starts with the construction of  $Vor(P)$  and its dual  $Del(P)$ . Each Voronoi vertex structure is equipped with the **label** and **visited** fields to keep track of the vertex label and the visited status during the incremental labeling. All the Voronoi vertices are initialized to *unvisited* in the beginning. Under dense sampling, extreme Voronoi vertices of infinite Voronoi edges induced by any pair of adjacent samples from pseudo-convex portions lie inside  $Cov(P)$ . This is established for  $\epsilon$ -sampling in Lemma 5.1, see Appendix. For convex portions, the convex hull is a linear approximation to the original curve and hence, these vertices also lie in the interior of the original curve. So, we label all such EVVs as *inner*. All the remaining Voronoi vertices are labelled *outer* at the start of the incremental labeling process. In the next step, a heap based priority queue, PQ of all the *outer* EVVs is created, where the EVVs are sorted in the descending order of the circumradii of the corresponding dual Delaunay triangles. In each

iteration, the algorithm picks the root element from  $PQ$  and apply the vertex labeling procedure given in Algorithm 1.

Once the incremental labeling has been applied to all the EVVs in  $PQ$ , it extracts the curve and MAT from  $Del(P)$  by employing  $Dual()$  function which gives the dual Delaunay edge of a Voronoi edge. The algorithm has been designed to address closed curves, and hence, we have avoided few conditions that may arise in the cases of open curves. Nevertheless, these additional conditions may be incorporated to extend the practical potentials of the proposed algorithm.

The number of Voronoi vertices is linear in terms of the point set size,  $n$ . Since each Voronoi vertex is visited exactly once in the  $IncrementalLabel()$  procedure, WHILE loop of Algorithm 2 costs only  $O(n)$ . Other operations such as label initialization, and curve and MAT extractions take linear time. As the number of EVVs are very low compared to the input samples,  $PQ$  creation and heapify costs are negligible. So, the worst case time complexity of the algorithm is  $O(n \log n + k \log k)$  where  $k = \#EVVs$ , and is mainly incurred due to the computation of Voronoi diagram.

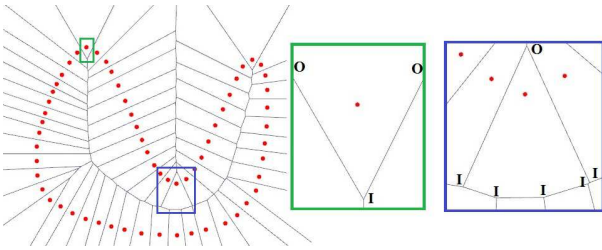


**Figure 8:** Different labeling patterns on the Voronoi cells of dominant points. Green and blue boxes depict examples of OIO and IOI patterns respectively.

### 3.4. Dominant Points Detection

The labeled Voronoi diagram obtained through the incremental labeling (Algorithm 1) can be further used to identify the points with high curvature values (or dominant points). We observe that a few of the vertices from the Voronoi cells of such points conform to interesting labeling patterns. The patterns are formed out of the labels of three consecutive Voronoi vertices along the Voronoi cell boundary, where each pattern consists of vertices with same labels at either side and a center vertex with a different label as shown in Figure 8. Since, the Voronoi vertices are labelled either as *inner* or *outer*, we have only two such labeling sequence referred to as IOI and OIO patterns (here, *inner* is abbreviated as I and *outer* is abbreviated as O). Under reasonably dense sampling along the curvature portions, which is often guaranteed in non-uniform sampling such as  $\epsilon$ -sampling, the Voronoi cells of points from curvature extremes tend to have either of IOI or OIO patterns on their Voronoi cells. This observation leads to a simple and immediate extraction scheme for DPs.

Input points with IOI or OIO patterns on their Voronoi cells are extracted as DPs subjected to one more constraints which filter out most of the false positives. We use a constraint similar to

the state transition rule (Definition 5). Let  $c, t_1, t_2$  be the central and the terminal vertices of an identified pattern (IOI or OIO) over the Voronoi cell of an input point  $p$ , respectively. We consider the line  $L$  going through  $p$  and orthogonal to the vector  $\vec{c\hat{p}}$ . The pattern and consequently the point is a qualified DP, if the central vertex  $c$  and the terminal vertices lie on either side of  $L$ . The DP extraction consists of a linear traversal over the Voronoi cells, a constant circular traversal over the vertices of a cell for identifying the discussed patterns and a constant time location check for the pattern vertices. Hence the time complexity of DP extraction is  $O(n \log n)$ , mainly due to Voronoi diagram computation.

## 4. Experimental Results

We implemented our algorithm in C++ using computational geometry algorithms library (CGAL). To evaluate the performance of our approach, we tested it on points sampled randomly from the contours of silhouettes from MPEG 7 CE Shape-1 Part B and aim@shape repositories. A few data sets were generated from the corresponding images using mesecina software [MGP07]. We compared our algorithm with other Delaunay/Voronoi based algorithms such as crust [ABE98], nearest neighbor crust [DK99], ec-shape [MPM15], shape-hull [PM15b], and the recent algorithms in [PM16] and [PMM18].

**Reconstruction from Sparse Data.** Sparse data represents a major challenge to any type of curve reconstruction algorithm, especially, when geometrical or topological information of the original curve is unknown. In practice, the proposed algorithm performed well for a variety of sparse and non-uniform input data as shown in Figure 9. For shapes such as the fish and the cup, the results generated by our algorithm and ec-shape [MPM15] are noticeably better as compared to the results of Delaunay based algorithms. Intuitively, the normal and tangent based vertex classification allows for a reasonably correct reconstruction even when the sampling is sparse.

In [PM15b], the authors propose shape-hull algorithm that reconstructs divergent concave curves and surfaces from their non-uniform samples. We would like to point out that our algorithms differ in the construction of curves. While the shape-hull algorithm [PM15b] constructs curves by repeatedly eliminating boundary Delaunay triangles subjected to circumcenter and regularity properties, the proposed algorithm relies on an incremental Voronoi vertex labeling based on the spatial distribution of Voronoi vertices with respect to the original curve portions approximated by the tangent lines at point samples. Further, [PM15b] has been tuned only for reconstruction, whereas the algorithm presented in this paper can also extract medial axis as well as dominant points. Compared to shape-hull, our algorithm nicely reconstructs divergent as well as non-divergent concave portions of closed curves as shown in Figure 10. Please note that the monkey point set has a non-divergent portion, which is well captured by our algorithm.

**Collection of Curves.** Our method also performs well in reconstructing a collection of closed curves from a sparsely sampled data as illustrated in the third row of Figure 9 and the top two rows in Figure 11. All the Voronoi vertices including a set of vertices between the samples of a pair of closed disconnected curves are

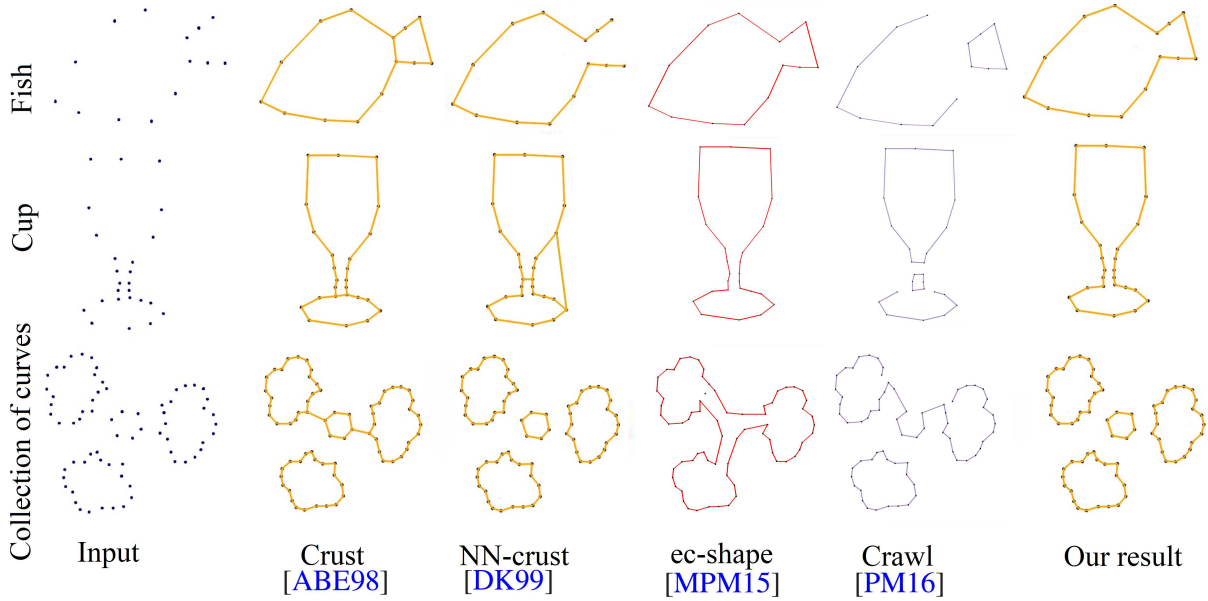


Figure 9: Reconstruction results of various algorithms on sparse data.

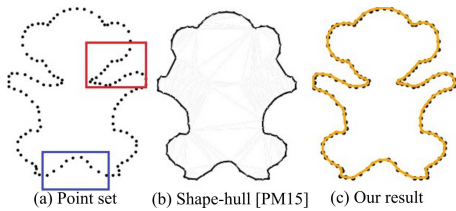


Figure 10: Reconstruction of monkey point set. In Figure 10(a), blue box contains a divergent concavity [PM15b] and red box encapsulates a non-divergent concavity.

classified as *outer* in the beginning of the algorithm. Incremental labeling on both the curves classify the interior Voronoi vertices as *inner* and as a consequence, the proposed algorithm is able to separate the collection of curves.

**Robustness to Outliers.** Most of the Delaunay/Voronoi based algorithms interpolate the input data and hence found to be intolerant towards outliers. For point sets having noise and outliers, curve fitting techniques may be considered a more appropriate choice. Curve fitting techniques, however make implicit assumptions on the underlying curve, which is highly impractical for sparse and non-uniform data. Since the incremental algorithm is also an interpolating technique, rather than eliminating the outliers from the results, we aim at showing the reconstruction of the original shape while retaining outliers in the scene. A post-processing step for denoising the output may be applied to eliminate outliers. Figure 11 (3-5 rows) visualizes a few more reconstruction results in the presence of outliers. The results clearly indicates the superiority of our algorithm in handling such inputs.

We experimented on a dove point set consisting of 54 points.

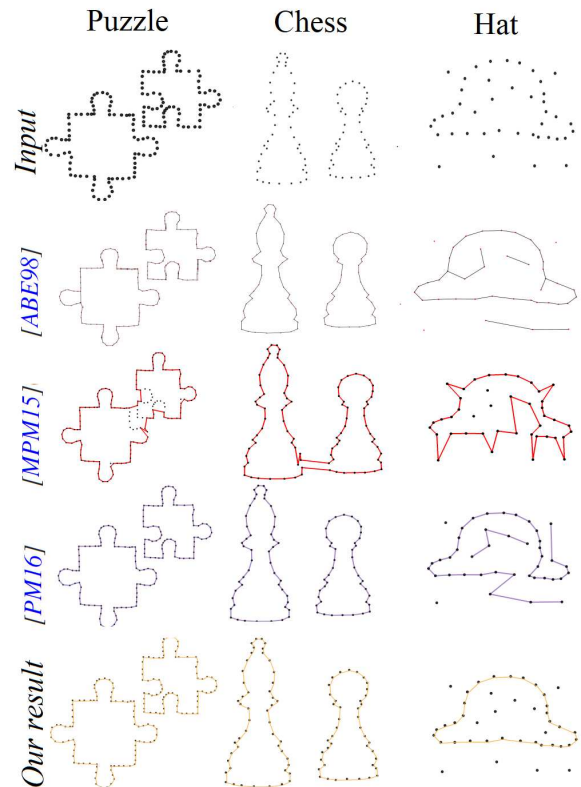
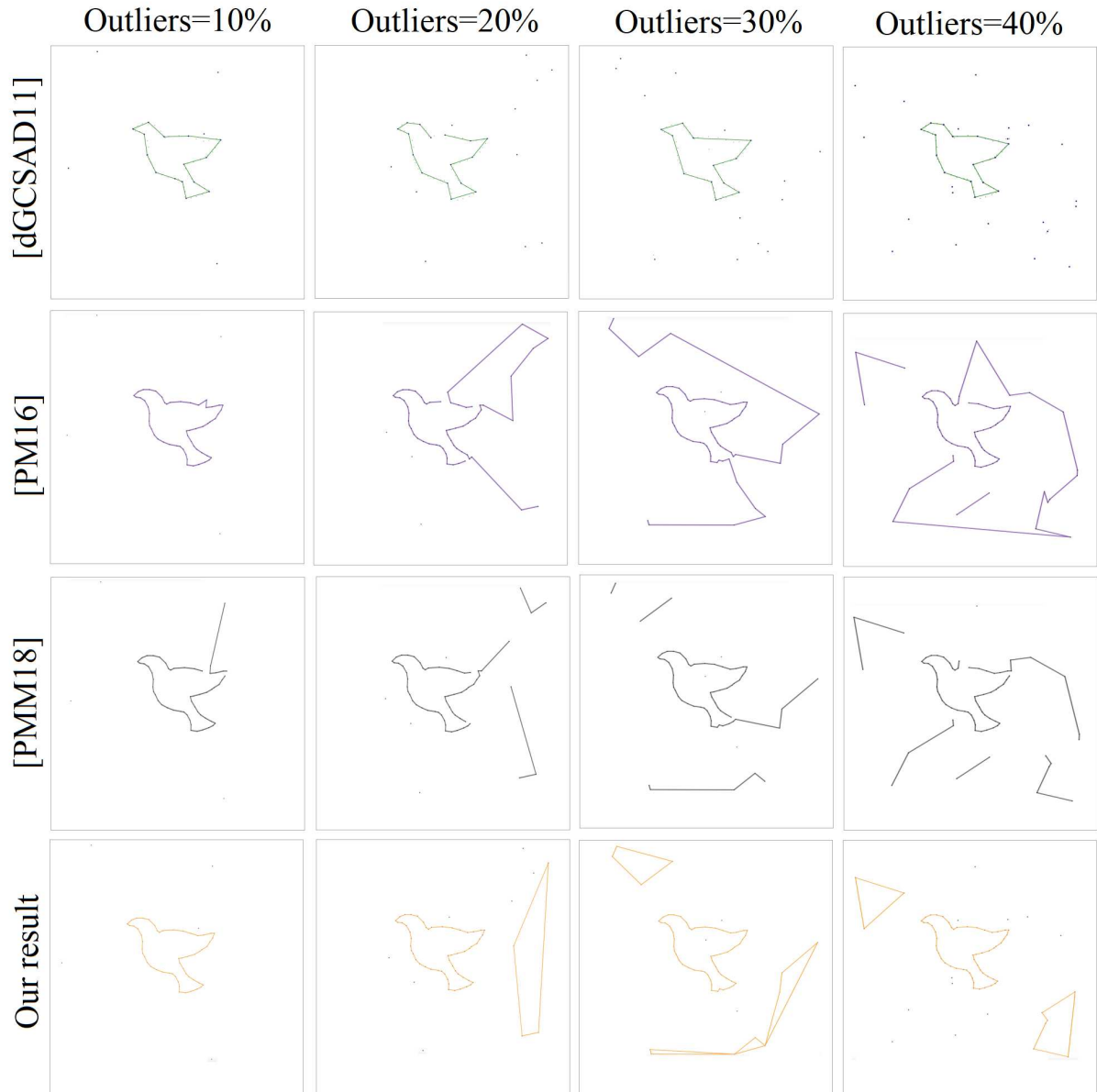


Figure 11: Reconstruction from collection of curves and curves in the presence of outliers.



**Figure 12: Outlier experiment:** All the stages of outlier injection, dove shape reconstructed by the proposed algorithm preserves fine details as compared to a simplified reconstruction by deGoes et al. [dGCSAD11] and the reconstruction with curve artifacts in [PM16] and [PMM18]. Outliers were generated using the software by deGoes et al. [dGCSAD11].

Random outliers, expressed as a percentage of the point set size, were injected to the input data as shown in Figure 12. Our approach is noticeably better at dealing with the outliers constituting even 40% of the curve sample. Results by deGoes et al. [dGCSAD11], loses many fine details of the dove shape even for 10% outliers. However, a few artifacts appear in the reconstruction for 40% outliers in all the algorithms. The reconstruction by [PM16] and [PMM18] produce curve artifacts. Please note that, albeit the artifacts, dove shape has been well reconstructed by our method. This is mainly due to the label transition failures which occur when the

incremental algorithm starts with EVVs induced fully or partially by the sparse outlier points. As a result, a continuous *inner* and *outer* combination of Voronoi vertices do not arise in the premise of outliers, thereby preventing them to be attached to the input curve.

**Dealing with Sharp Corners.** On closed and concave curves with sharp corners, our approach performs better than other methods. For instance, the left horn of oni which is sharp and pointed in Figure 13 is well captured by our algorithm as opposed to other crust algorithms. Though optimal transport based approach recon-

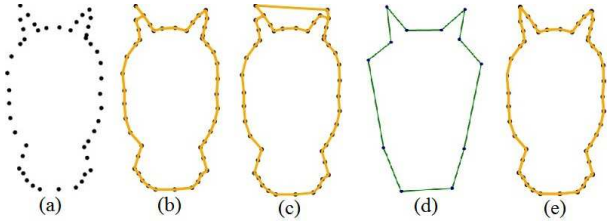


**Figure 13:** Reconstruction of oni data. (a) Point set (b) crust [ABE98] (c) nearest neighbor crust [DK99] (d) result of [dGCSAD11] (e) our result.

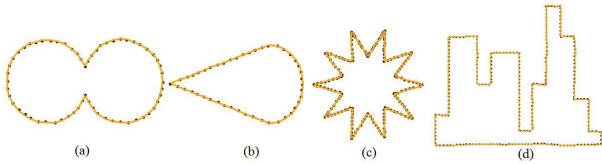


**Figure 14:** Results of curves with sharp features.

structs both the sharp corners well, it loses several other details such as neck of the oni. In contrast, our method not only captures the sharp corners but also preserves other details of the original curve. We would like to remark that a few work [DW02, Gie99, FR01] specially designed to work on sharp corners are expected to possibly capture the correct boundary of Oni data.

Figure 14 shows our results for point sets with sharp features. The incremental algorithm correctly reconstructs the shapes for point sets in Figures 14 (a)-(b), for which all the TSP based algorithms listed in [AMNS00] fail.

**Quantitative Analysis.** We evaluate our algorithm quantitatively using  $L^2$ -error norm measure on the points sampled from the borders of various countries.  $L^2$ -error norm is the area of the symmetric difference between the original shape  $O$  and the reconstructed shape as a proportion of the total area of the original shape  $O$  [PM15a]. An zero value for  $L^2$ -error norm implies that the two shapes are equal in area and also their boundaries are aligned perfectly over each other. Fig. 15 visualizes the symmetric difference ( $L^2$ -error) for the Luxemburg country shape with varying point densities. Fig. 16 shows the  $L^2$ -error metric of various algorithms for varying point densities of different country shapes. Compared to the competitors, the proposed algorithm performed well for most of the country shapes. Please note that the test shapes were chosen based on the sinusoidal characteristics of the boundaries. A qualitative comparison of the performance of various algorithms with respect to the  $L^2$ -error metric on Zambia shape is presented in Fig. 17. Compared to the other three methods in the figure, the proposed algorithm is very successful in capturing the concavities of the shape, even for the sparse input, as quantified in Fig 16(d).

**Medial Axis Results:** Figure 18 shows the reconstructed curves as well as the medial axes for various non-uniformly sampled data. Like any other approach, the approximation quality of our medial axis algorithm is limited by the sampling density of input data and the smoothness of the given curve. For a qualitative comparison,

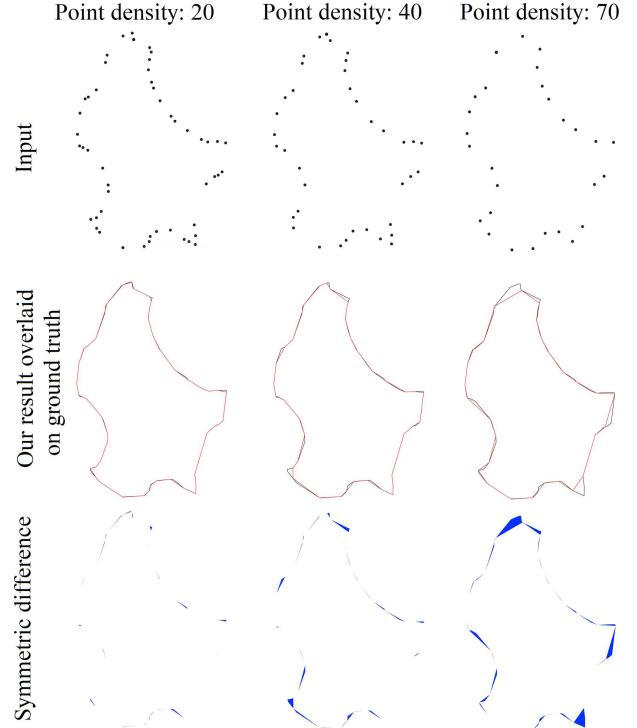


**Figure 15:** Illustration of  $L^2$ -error metric.

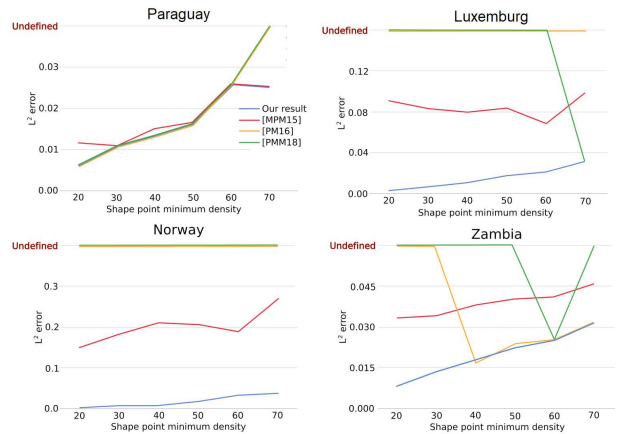


**Figure 16:** Variation in the accuracy of reconstruction (quantified in terms of  $L^2$ -error metric) with the changing sample density of various inputs.

we have also presented the MAT results of local crust [Gol99] algorithm. For the given inputs, both the algorithms generated the same MATs. The results seem reasonable as both these algorithms perform MAT extraction on the underlying labelled Voronoi vertices, however, the labeling procedure differs considerably (see [Gol99] for details).

**Dominant Points of Different Data Sets:** Figure 19 shows the dominant points (blue circles) and the approximated polygons of

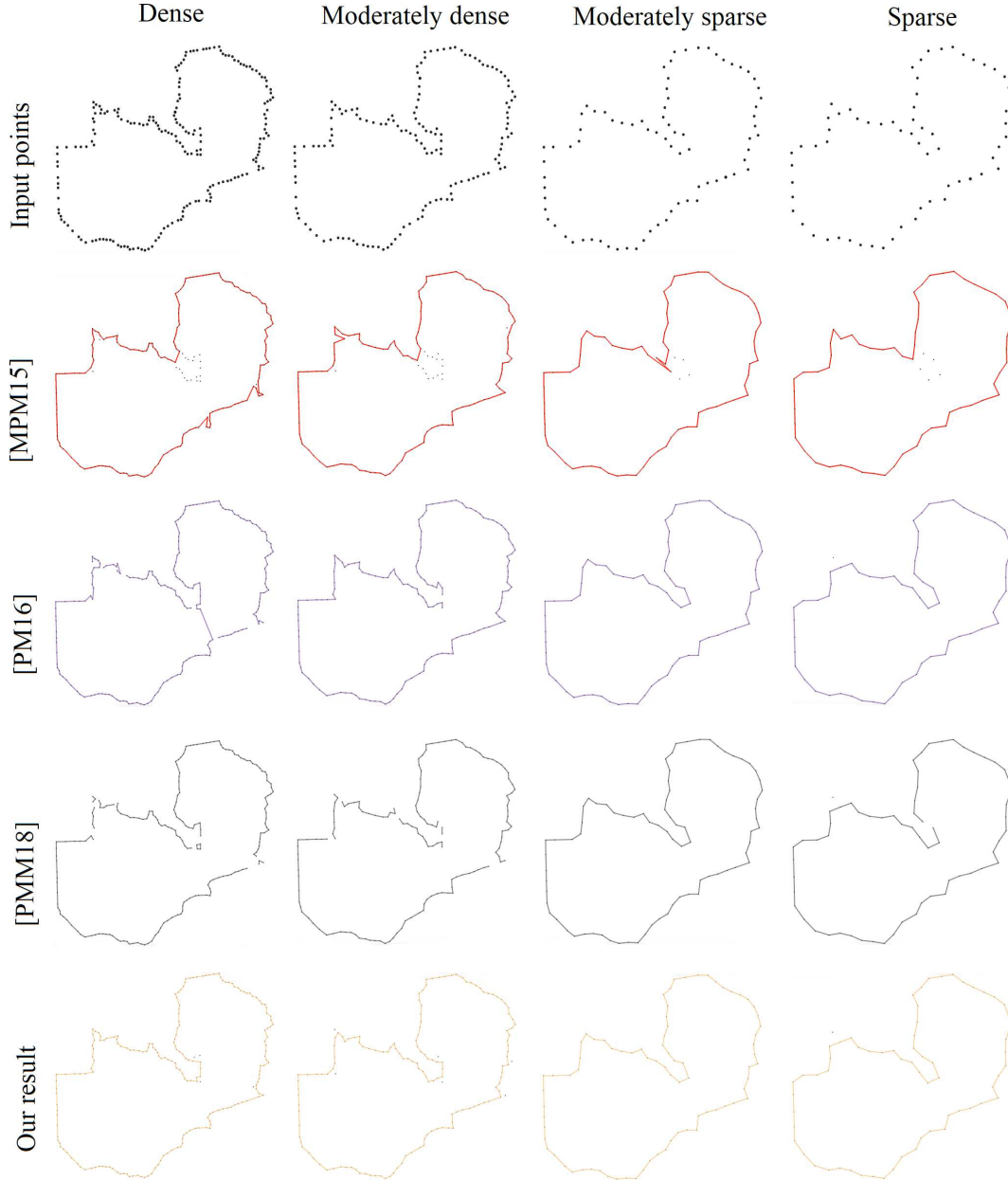


**Figure 17:** A qualitative comparison of the curve reconstruction algorithms for Zambia point set with varying sampling densities. See Fig. 16(d) for the quantitative results.

various point sets. Polygons are approximated from the dominant points ordered along the original contour. Usually, polygonal approximation algorithms on digital curves are evaluated using metrics such as compression ratio ( $CR = \frac{\#input\ points}{\#dominant\ points}$ ), integral square error (ISE), i.e., sum of squared distances of the curve points from approximating polygon or figure of merit ( $FOM = \frac{CR}{ISE}$ ). In our setting, which is mainly intended for extraction of shape structures from non-uniform points rather than digital curves, we resort to an evaluation based on qualitative analysis and the compression ratio. Moreover, the curves reconstructed by our algorithm maintains no

information on the vertex ordering along the curve which makes it difficult to compute ISE values even if the ground truths are available.

The demonstrated results in Figure 19 indicate that the proposed framework is capable of detecting DPs at significant locations on the contours and consequently, generating polygons that preserve the morphology of the shape with a reasonable accuracy. However, for benchmark data such as chromosome and infinity, algorithms [RR93, Wu03] perform better than the proposed method in terms of

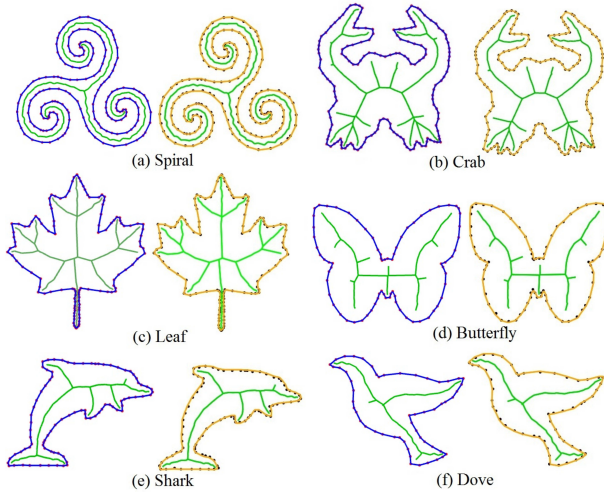


**Figure 18: Medial Axes Gallery:** MAT generated for various non-uniformly sampled data by Local crust [Gol99](column 1) and our algorithm (column 2).

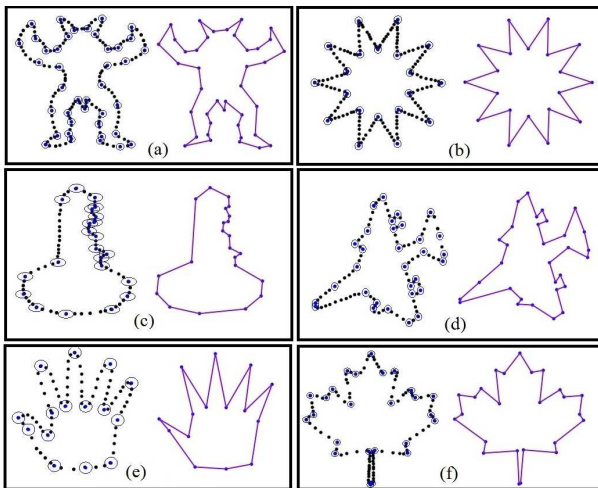


**Figure 19:** Dominant points and the approximated polygons of various point sets. (a) Armadillo ( $CR=4.18$ ) (b) Star ( $CR=8.65$ ) (c) Key ( $CR=3.64$ ) (d) Aeroplane ( $CR=3.26$ ) (e) Hand ( $CR=5.73$ ) and (f) Leaf ( $CR=4.52$ ). Points in each set are ordered in counter-clockwise direction and the polygons are reconstructed by simply connecting these ordered points.

FOM as shown in Table 1 and Figure 20. Our method still detects most of the DPs of these benchmarks. Our experimental study and comparison reveals that the proposed DP detection scheme is more suitable for non-uniformly sampled data with a high sampling rate along the high curvature portions of the contours as shown in Figure 19.

Shape	Method	#DP	CR	ISE	FOM
Chromosome (n=60)	[RR93]	18	3.33	5.57	0.6
	[Wu03]	17	3.53	5.01	0.7
	Our method	21	2.85	25.35	0.1
Infinity (n=45)	[RR93]	12	3.75	5.99	0.6
	[Wu03]	13	3.46	5.17	0.7
	Our method	24	1.88	4.43	0.4

**Table 1:** Statistical results of dominant point detection by different algorithms. FOM values are truncated to one decimal place. A relatively high value of ISE for the chromosome is caused due to the lower pocket as highlighted in Figure 20.

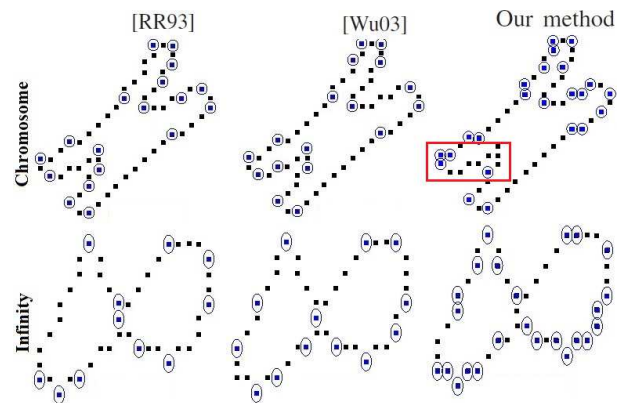


**Figure 20:** Dominant points of benchmark data detected by various algorithms.

## 5. Conclusion

In this paper, we presented a multi-purpose Voronoi and Delaunay based framework for curve reconstruction, medial axis approximation and dominant point detection. The key part of the framework is a simple incremental technique that classifies the Voronoi vertices into *outer* and *inner* with respect to the original curve. Under  $\epsilon$ -sampling model, it has been established that the incremental algorithm constructs a piece-wise linear approximation to smooth, closed and planar curves. Experimental results indicate that our approach is capable of reconstructing curves from sparse data. It also handles collection of curves successfully, and captures sharp corners, though the algorithm is designed for smooth and closed curves. In the Delaunay/Voronoi based domain, only algorithms such as conservative crust [DMR00] handles outliers, however at the expense of parameter tuning. As opposed to this, our algorithm found to perform well in the case of curves with outliers without using any external parameter. In future, one can work on extending the framework for the reconstruction of multiply connected curves with a hierarchical incremental labeling.

## References

- [AB98] AMENTA N., BERN M.: Surface reconstruction by voronoi filtering. In *Proceedings of the Fourteenth Annual Symposium on Computational Geometry* (New York, NY, USA, 1998), SCG '98, ACM, pp. 39–48. 5, 6
- [ABE98] AMENTA N., BERN M., EPPSTEIN D.: The crust and the beta-skeleton: Combinatorial curve reconstruction. In *Graphical Models and Image Processing* (1998), pp. 125–135. 2, 3, 4, 7, 10, 14, 15
- [ACK01] AMENTA N., CHOI S., KOLLURI R. K.: The power crust, unions of balls, and the medial axis transform. *Computational Geometry* 19, 2-3 (2001), 127 – 153. Combinatorial Curves and Surfaces. 2, 3
- [AK01] AMENTA N., KOLLURI R. K.: The medial axis of a union of balls. *Computational Geometry* 20, 1-2 (2001), 25 – 37. 3
- [AM97] ATTALI D., MONTANVERT A.: Computing and simplifying 2d and 3d continuous skeletons. *Computer Vision and Image Understanding* 67, 3 (1997), 261 – 273. 3
- [AM01] ALTHAUS E., MEHLHORN K.: Traveling salesman-based curve reconstruction in polynomial time. *SIAM Journal on Computing* 31, 1 (2001), 27–66. 2
- [AMNS00] ALTHAUS E., MEHLOHRN K., NAHER S., SCHIRRA S.: Experiments on curve reconstruction. In *Proceedings of 2nd Workshop on Algorithms Engineering experiments* (2000), pp. 104–114. 10
- [Att54] ATTNEAVE F.: Some informational aspects of visual perception. *Psychological Review* 61, 3 (May 1954), 183–193. 3
- [Att98] ATTALI D.:  $r$ -regular shape reconstruction from unorganized points. *Computational Geometry* 10, 4 (1998), 239 – 247. 2
- [BA92] BRANDT J. W., ALGAZI V.: Continuous skeleton computation by voronoi diagram. *CVGIP: Image Understanding* 55, 3 (1992), 329 – 338. 3
- [Bra94] BRANDT J.: Convergence and continuity criteria for discrete approximations of the continuous planar skeleton. *CVGIP: Image Understanding* 59, 1 (1994), 116 – 124. 3
- [CFG\*05] CHENG S.-W., FUNKE S., GOLIN M., KUMAR P., POON S.-H., RAMOS E.: Curve reconstruction from noisy samples. *Computational Geometry* 31, 1-2 (2005), 63 – 100. 2
- [dGCSAD11] DE GOES F., COHEN-STEINER D., ALLIEZ P., DESBRUN M.: An optimal transport approach to robust reconstruction and simplification of 2d shapes. *Computer Graphics Forum* 30, 5 (2011), 1593–1602. 2, 9, 10
- [DK99] DEY T. K., KUMAR P.: A simple provable algorithm for curve reconstruction. In *Proceedings of the Tenth Annual ACM-SIAM Symposium on Discrete Algorithms* (1999), SODA '99, pp. 893–894. 2, 7, 10
- [DMR00] DEY T. K., MEHLHORN K., RAMOS E. A.: Curve reconstruction: Connecting dots with good reason. *Computational Geometry* 15, 4 (2000), 229 – 244. 2, 12
- [Dun86] DUNHAM J. G.: Optimum uniform piecewise linear approximation of planar curves. *IEEE Trans. Pattern Anal. Mach. Intell.* 8, 1 (1986), 67–75. 3
- [DW01] DEY T. K., WENGER R.: Reconstructing curves with sharp corners. *Computational Geometry* 19, 2-3 (2001), 89 – 99. 2, 5
- [DW02] DEY T. K., WENGER R.: Fast reconstruction of curves with sharp corners. *International Journal of Computational Geometry & Applications* 12, 05 (2002), 353–400. 2, 10
- [EKS83] EDELSBRUNNER H., KIRKPATRICK D., SEIDEL R.: On the shape of a set of points in the plane. *Information Theory, IEEE Transactions on* 29, 4 (jul 1983), 551 – 559. 2
- [FEC02] FABBRI R., ESTROZIL F., COSTA L. F.: On voronoi diagrams and medial axes. *Journal of Mathematical Imaging and Vision* 17 (2002), 27–40. 3
- [FR01] FUNKE S., RAMOS E. A.: Reconstructing a collection of curves with corners and endpoints. In *Proceedings of the Twelfth Annual ACM-SIAM Symposium on Discrete Algorithms* (2001), SODA '01, pp. 344–353. 2, 10
- [GDN04] GURU D., DINESH R., NAGABHUSHAN P.: Boundary based corner detection and localization using new 'cornerity' index: a robust approach. In *Computer and Robot Vision, 2004. Proceedings. First Canadian Conference on* (May 2004), pp. 417–423. 3
- [Gie99] GIESEN J.: Curve reconstruction, the traveling salesman problem and menger's theorem on length. In *Proceedings of the Fifteenth Annual Symposium on Computational Geometry* (New York, NY, USA, 1999), SCG '99, ACM, pp. 207–216. 2, 10
- [GMP07a] GIESEN J., MIKLOS B., PAULY M.: Medial axis approximation of planar shapes from union of balls: A simpler and more robust algorithm. In *CCCG* (2007), Bose P., (Ed.), pp. 105–108. 3
- [GMP07b] GIESEN J., MIKLOS B., PAULY M.: Medial axis approximation of planar shapes from union of balls: A simpler and more robust algorithm. In *Proceedings of the 19th Annual Canadian Conference on Computational Geometry, CCCG 2007, August 20-22, 2007, Carleton University, Ottawa, Canada* (2007), pp. 105–108. 6, 16
- [Gol99] GOLD C.: Crust and anti-crust: A one-step boundary and skeleton extraction algorithm. In *Proceedings of the Fifteenth Annual Symposium on Computational Geometry* (New York, NY, USA, 1999), SCG '99, ACM, pp. 189–196. URL: <http://doi.acm.org/10.1145/304893.304971>, doi:10.1145/304893.304971. 2, 3, 6, 10, 12
- [HAA94] HELD A., ABE K., ARCELLI C.: Towards a hierarchical contour description via dominant point detection. *Systems, Man and Cybernetics, IEEE Transactions on* 24, 6 (Jun 1994), 942–949. 3
- [HS99] HUANG S.-C., SUN Y.-N.: Polygonal approximation using genetic algorithms. *Pattern Recognition* 32, 8 (1999), 1409 – 1420. 3
- [KD82] KUROZUMI Y., DAVIS W. A.: Polygonal approximation by the minimax method. *Computer Graphics and Image Processing* 19, 3 (1982), 248 – 264. 3
- [Lee00] LEE I.-K.: Curve reconstruction from unorganized points. *Computer Aided Geometric Design* 17, 2 (2000), 161 – 177. 1, 2
- [LWS\*15] LI P., WANG B., SUN F., GUO X., ZHANG C., WANG W.: Qmat: Computing medial axis transform by quadratic error minimization. *ACM Trans. Graph.* 35, 1 (Dec. 2015), 8:1–8:16. 3
- [Mas08] MASOOD A.: Optimized polygonal approximation by dominant point deletion. *Pattern Recognition* 41, 1 (2008), 227 – 239. 3
- [MBS16] M. BERGER ANDREA TAGLIASACCHI L. S. P. A. G. G. J. L. A. S., SILVA C.: A survey of surface reconstruction from point clouds. *Computer Graphics Forum'16 (extended journal version of the EG STAR)* (2016). 1
- [MGP07] MIKLOS B., GIESEN J., PAULY M.: Medial axis approximation from inner voronoi balls: A demo of the mesecina tool. In *Proceedings of the Twenty-third Annual Symposium on Computational Geometry* (New York, NY, USA, 2007), SCG '07, ACM, pp. 123–124. 7
- [MPM15] METHIRUMANGALATH S., PARAKKAT A. D., MUTHUGANAPATHY R.: A unified approach towards reconstruction of a planar point set. *Comput. Graph.* 51, C (Oct. 2015), 90–97. 2, 7
- [MS03] MARJI M., SIY P.: A new algorithm for dominant points detection and polygonization of digital curves. *Pattern Recognition* 36, 10 (2003), 2239 – 2251. 3
- [OM13] OHRHALLINGER S., MUDUR S. P.: An efficient algorithm for determining an aesthetic shape connecting unorganized 2d points. *Comput. Graph. Forum* 32, 8 (2013), 72–88. 2
- [OMW16] OHRHALLINGER S., MITCHELL S., WIMMER M.: Curve reconstruction with many fewer samples. *Computer Graphics Forum* 35, 5 (2016), 167–176. 2

- [O'R98] O'ROURKE J.: *Computational Geometry in C*, 2nd ed. Cambridge University Press, New York, NY, USA, 1998. 4
- [OW18] OHRHALLINGER S., WIMMER M.: Fitconnect: Connecting noisy 2d samples by fitted neighborhoods. *Computer Graphics Forum*, Early view (Apr. 2018). 2
- [PM15a] PEETHAMBARAN J., MUTHUGANAPATHY R.: A non-parametric approach to shape reconstruction from planar point sets through delaunay filtering. *Computer-Aided Design* 62 (2015), 164 – 175. 10
- [PM15b] PEETHAMBARAN J., MUTHUGANAPATHY R.: Reconstruction of water-tight surfaces through delaunay sculpting. *Computer-Aided Design* 58, 0 (2015), 62 – 72. 7, 8
- [PM16] PARAKKAT A. D., MUTHUGANAPATHY R.: Crawl through neighbors: A simple curve reconstruction algorithm. *Computer Graphics Forum* 35, 5 (2016), 177–186. 2, 7, 9
- [PMM18] PARAKKAT A. D., METHIRUMANGALATH S., MUTHUGANAPATHY R.: Peeling the longest: A simple generalized curve reconstruction algorithm. *Computers & Graphics* 74 (2018), 191 – 201. 7, 9
- [PNK98] PAL N. R., NANDI S., KUNDU M. K.: Self-crossover-a new genetic operator and its application to feature selection. *Int. J. Systems Science* 29, 2 (1998), 207–212. 3
- [PPM15] PEETHAMBARAN J., PARAKKAT A., MUTHUGANAPATHY R.: A voronoi based labeling approach to curve reconstruction and medial axis approximation. In *Pacific Graphics 2015* (October 2015), Eurographics Digital Library. 2, 3
- [Ram72] RAMER U.: An iterative procedure for the polygonal approximation of plane curves. *Computer Graphics and Image Processing* 1, 3 (1972), 244 – 256. 3
- [RR93] RAY B. K., RAY K. S.: Determination of optimal polygon from digital curve using  $\{L1\}$  norm. *Pattern Recognition* 26, 4 (1993), 505 – 509. 3, 11, 12
- [Sat92] SATO Y.: Piecewise linear approximation of plane curves by perimeter optimization. *Pattern Recognition* 25, 12 (1992), 1535 – 1543. 3
- [TC89] TEH C.-H., CHIN R.: On the detection of dominant points on digital curves. *Pattern Analysis and Machine Intelligence, IEEE Transactions on* 11, 8 (Aug 1989), 859–872. 3
- [TDS\*16] TAGLIASACCHI A., DELAME T., SPAGNUOLO M., AMENTA N., TELEA A.: 3d skeletons: A state-of-the-art report. *Computer Graphics Forum (Proc. Eurographics)* (2016). 3
- [Wan14] Robust reconstruction of 2d curves from scattered noisy point data. *Computer-Aided Design* 50, 0 (2014), 27 – 40. 1, 2
- [Wu02] WU W.-Y.: A dynamic method for dominant point detection. *Graphical Models* 64, 5 (2002), 304 – 315. 3
- [Wu03] WU W.-Y.: An adaptive method for detecting dominant points. *Pattern Recognition* 36, 10 (2003), 2231 – 2237. 11, 12
- [YIN99] YIN P.-Y.: Genetic algorithms for polygonal approximation of digital curves. *International Journal of Pattern Recognition and Artificial Intelligence* 13, 07 (1999), 1061–1082. 3
- [ZC18] ZHONG Y., CHEN F.: Computing medial axis transformations of 2d point clouds. *Graphical Models* 97 (2018), 50 – 63. 3
- [ZSC\*14] ZHU Y., SUN F., CHOI Y.-K., JÄNTTLER B., WANG W.: Computing a compact spline representation of the medial axis transform of a 2d shape. *Graphical Models* 76, 5 (2014), 252 – 262. Geometric Modeling and Processing 2014. 3

## Appendix

In Appendix, we provide a few theoretical analysis and observation about the proposed algorithm. Primarily, we aim to prove that the

reconstructed curve consists of only the edges between adjacent samples of  $\mathcal{C}$ . To argue for the correct reconstruction, we consider convex ( $\mathcal{C}_{cvx}$ ) and concave ( $\mathcal{C}_{cv}$ ) portions separately.

**Pseudo-convex portions:** To achieve correct reconstruction of  $\mathcal{C}_{cvx}$ , all the finite Voronoi vertices, of infinite edges corresponding to the adjacent samples from  $\mathcal{C}_{cvx}$ , must lie interior to  $Conv(P)$ . We establish this claim in Lemma 5.1.

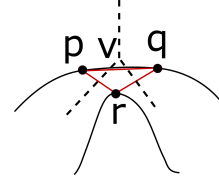


Figure 21: (a) Illustration of Lemma 5.1.

**LEMMA 5.1** In  $Vor(P)$ , where  $P$  is  $\epsilon$ -sampled from  $\mathcal{C}$ , EVVs of infinite edges between the adjacent samples of the pseudo-convex portions from  $\mathcal{C}_{cvx}$ , lie interior to  $Conv(P)$

*Proof* Consider two adjacent samples  $p, q \in P$  from a pseudo-convex portion  $C \in \mathcal{C}_{cvx}$  (refer to Figure 21) that lie at a maximum distance of  $d(p, q) = \epsilon lfs(p)$ . Let  $v$  be the finite Voronoi vertex of the infinite edge between  $p$  and  $q$ . We assume the contrary. i.e.  $v$  lies outside  $Conv(P)$ . Let  $r \in P$  be a sample from  $\mathcal{C}$  that induces  $v$ . As  $v$  lies outside  $Conv(P)$ , the sample  $r$  must be non-adjacent to either  $p$  or  $q$  along the curve. As  $v$  lies outside  $Conv(P)$ , it also lies outside the edge  $(p, q) \in Conv(P)$  thereby making the  $\triangle pqr$  obtuse at  $r$ . Consequently,  $d(p, q) > d(p, r)$ . This implies that a non-adjacent (along the curve) sample  $r$  lies within a sampling distance of  $\epsilon lfs(s)$  for the sample  $p$ . This is a contradiction to the definition of  $\epsilon$ -sampling and hence the lemma.  $\square$

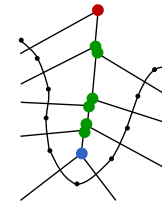
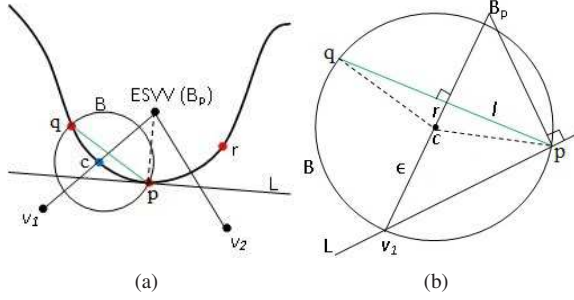


Figure 22: Illustration of different SVVs in a pseudo concavity. Red, green and blue dots represent EVV, middle SVVs and end SVV respectively.

**Pseudo concavities:** The crucial part of the correctness proof lies in establishing the faithful reconstruction of pseudo concavities. Each pseudo concavity has a branch line consisting of EVV, middle SVVs and end SVVs as shown in Figure 22. Usually, a main branch line starts with a EVV and a sub branch line starts with a middle SVV. A middle SVV can have either two or three adjacent outer Voronoi vertices. An end SVV is a Voronoi vertex whose two branching Voronoi edges are shared by three adjacent samples  $p, q, r \in P$  from  $\mathcal{C}$  (refer to Figure 23(a)).

We consider a curve Voronoi disk [ABE98]  $B$  of radius  $\epsilon$  passing through two adjacent points  $p, q \in P$  sampled from  $\mathcal{C}$  (refer to



**Figure 23:** (a) Construction for Lemma 5.2 (b) A contradicting case for Lemma 5.2.

Figure 23(b)). Without loss of generality, we assume the local feature size of the center of  $B$  to be 1 ( $lfs(c) = 1$ ). Due to Lemma 9 of [ABE98], we know that the angle formed by  $p$  and  $q$  at the curve Voronoi vertex  $c$  is  $\pi - 2\arcsin\frac{\epsilon}{2}$ . Let  $B_p v_1$  be the bisector of the chord  $qp$ . From Figure 23(b), it is easy to verify the following:

1.  $l = \frac{\epsilon}{2}\sqrt{4-\epsilon^2}$
2.  $r = \frac{\epsilon^2}{2}$
3.  $\angle qcv_1 = \frac{\pi}{2} + \arcsin(\frac{\epsilon}{2})$
4.  $\angle qpv_1 = \arctan(\frac{2+\epsilon}{\sqrt{4-\epsilon^2}})$

Next, few lemmas have been proved under the assumption that the Voronoi cell  $V_p$  is a part of VD induced by a set of points  $\epsilon$ -sampled from  $C$ .

**LEMMA 5.2** End SVV and the other Voronoi vertices of  $V_p$ , lie on either side of the line  $L$  perpendicular to  $\overline{B_p p}$  for  $\epsilon \leq 0.4$

*Proof* In Theorem 14 of [ABE98], Amenta et al. showed that curve Voronoi disks [ABE98] do not contain any vertices of  $Vor(P)$  for  $\epsilon \leq 0.4$ . We adapt their theorem to our algorithmic conditions and establish the lemma (Refer to Figure 23 for an illustration). Consider three adjacent samples  $p, q, r$  from a pseudo concavity of  $C_{ccv}$  that induce an end source vertex  $B_p$ . Let  $e_1 = (B_p, v_1)$  and  $e_2 = (B_p, v_2)$  are the Voronoi bisectors of  $p, q$  and  $p, r$ , respectively. Let  $B$  be a curve Voronoi disk passing through samples  $p$  and  $q$  which is centered at the curve Voronoi vertex [ABE98]  $c$ . We show that  $B_p$  and  $v_1$  lie on either side of  $L$ , where  $L$  is the line passing through  $p$  orthogonal to  $\overline{B_p q}$ .

Theorem 14 of [ABE98] implies that  $v_1$  can move only along the boundary or outside of  $B$ . Assume the case where  $v_1$  approaches the sample  $p$  along the boundary of  $B$ .  $v_1$  crosses  $L$  only after coinciding with the sample  $p$ , during which, the line  $e_1$  becomes a non-bisector of  $p$  and  $q$ . This contradicts our assumption on  $e_1$ . Similarly, consider the case where  $v_1$  approaches the sample  $q$  along the boundary of  $B$ . Suppose, it coincides with the point of intersection of  $L$  with  $\partial B$  on its way as shown in Figure 23(b). The angle subtended by the chord  $qv_1$  at the point  $p$  must be half the central angle ( $\angle qcv_1$ ) subtended by it. i.e.  $\angle qpv_1 = \frac{1}{2}\angle qcv_1$ . On substituting the values for  $r$  and  $l$  from Figure 23(b), we get the Equation 1.

$$\arctan\left(\frac{2+\epsilon}{\sqrt{4-\epsilon^2}}\right) = \frac{1}{2}\left(\frac{\pi}{2} + \arcsin\left(\frac{\epsilon}{2}\right)\right) \quad (1)$$

We can observe that the Equation 1 does not hold for any values of  $\epsilon$  in the interval  $[0, 1]$  (consequently for  $\epsilon \in [0, 0.4]$ ). Hence, vertex  $v_1$  can not merge with the point of intersection of  $L$  and  $\partial B$  on its way to  $q$ . Further, it can not move nearer to  $q$  as it violates the assumption that it orthogonally bisects the chord  $pq$  of  $B$ . Hence,  $v_1$  can lie only on or outside  $\partial B$  in the half plane opposite to the one that containing  $B_p$ . Similar arguments hold for the vertex  $v_2$  as well and hence the lemma.  $\square$

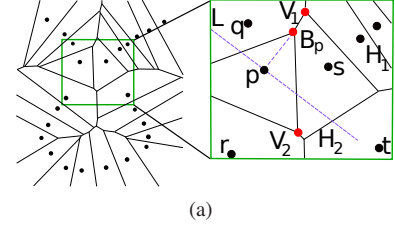


**Figure 24:** Illustration showing the existence of active Voronoi vertices in pseudo-concavities.

To show the existence of outer Voronoi vertices in pseudo-concavities, we consider the construction in the inset of Figure 24. It consists of five samples three of which  $q, p, r$  are adjacent, Voronoi cell  $V_p$  of a sample  $p \in P$ , its SVV ( $B_p$ ) and Voronoi vertices  $v_1$  and  $v_2$  adjacent to  $B_p$  lying in the pseudo concave region. The samples  $s, t$  are adjacent to each other and non-adjacent to  $p, q, r$ . Let  $L$  be the line orthogonal to  $\overline{B_p p}$ . We need to show that  $v_2$  lies in the half plane containing  $B_p$  with respect to  $L$ . It is obvious from the Figure 24 that  $v_2$  is either induced by  $\triangle psr$  or  $\triangle pst$ . For the sake of argument, we assume that  $v_2$  is a Voronoi vertex induced by samples  $p, s$  and  $r$ .

Since we need the half planes to be unchanging, we will fix the samples  $q, p, s$  and analyze the effect of the location of  $v_2$  on  $r$ . As  $v_2$  moves away from  $L$  in  $H_2$ ,  $r$  also tends to move apart from the samples  $p$  and  $s$ . This will ultimately cause a violation on  $\epsilon$ -sampling as it is evident that  $d(p, r)$  will be greater than  $d(p, s)$  and  $s$  is a non-adjacent sample of  $p$ . So, under a sufficiently dense sampling,  $v_2$  always tends to lie on or away from  $L$  in  $H_1$ . A similar argument holds good if we consider that  $v_2$  is induced by  $\triangle pst$ .

**PROPOSITION 5.3** The curve reconstructed by the incremental algorithm for a finite set of points  $P$ , where  $P$  is  $\epsilon$ -sampled from a smooth, closed and planar curve  $C$ , contains an edge between every pair of adjacent samples of  $C$ , for  $\epsilon < 0.4$

*Proof* We argue for the piece-wise linear reconstruction of  $C_{cvx}$  and  $C_{ccv}$ . Due to Lemma 5.1, all the finite Voronoi vertices on the infinite edges corresponding to adjacent samples from  $C_{cvx}$  are labelled outer and subsequently the algorithm constructs a piece-wise linear approximation to  $C_{cvx}$ . We know that there exists at least one finite Voronoi vertex corresponding to each pseudo concavity outside  $Conv(P)$  (Lemma 3.1) and hence the labeling happens for each pseudo concavity of  $C$ . Lemma 5.2 ensures that the edges between the adjacent samples in the pseudo concavities have outer and inner Voronoi vertices. Further, it ensures that the labeling does not get into the interior of  $C$ . Finally, existence of a proper branch line that covers the entire pseudo concavity is captured in Figure 24. We

conclude that under sufficiently dense sampling, the reconstructed curve represents a piece-wise linear approximation to  $\mathcal{C}$ , where  $\mathcal{C}$  is a smooth, closed planar curve.  $\square$

**Medial axis:** As a consequence of the Proposition 5.3, the curve reconstructed by the proposed algorithm represents a piece-wise linear representation to  $\mathcal{C}$ . All the inner Voronoi vertices represents the centers of the interior Voronoi disks. In [GMP07b], the authors established that the MA of  $\mathcal{C}$  can be approximated from the centers of the interior Voronoi disks of  $Vor(P)$  where  $P$  is  $\epsilon$ -sampled from  $\mathcal{C}$  for certain  $\epsilon < 0.207$ . Since MAT is an approximation from the centers of interior Voronoi disks, the theory is equally applicable to our medial axis approximation for concave and closed curves.